UCSF

UC San Francisco Previously Published Works

Title

Adipocyte JAK2 Regulates Hepatic Insulin Sensitivity Independently of Body Composition, Liver Lipid Content, and Hepatic Insulin Signaling

Permalink

Journal

ISSN

Authors

Corbit, Kevin C
Camporez, João Paulo G
Edmunds, Lia R
et al.

Publication Date

DOI

Adipocyte JAK2 Regulates Hepatic Insulin Sensitivity Independently of Body Composition, Liver Lipid Content, and Hepatic Insulin Signaling

Kevin C. Corbit,[1] João Paulo G. Camporez,[2] Lia R. Edmunds,[3] Jennifer L. Tran,[1] Nicholas B. Vera,[4] Derek M. Erion,[4] Rahul C. Deo,[1] Rachel J. Perry,[2] Gerald I. Shulman,[2,5,6] Michael J. Jurczak,[3] and Ethan J. Weiss[1]

Disruption of hepatocyte growth hormone (GH) signaling through disruption of *Jak2* (JAK2L) leads to fatty liver. Previously, we demonstrated that development of fatty liver depends on adipocyte GH signaling. We sought to determine the individual roles of hepatocyte and adipocyte *Jak2* on whole-body and tissue insulin sensitivity and liver metabolism. On chow, JAK2L mice had hepatic steatosis and severe whole-body and hepatic insulin resistance. However, concomitant deletion of *Jak2* in hepatocytes and adipocytes (JAK2LA) completely normalized insulin sensitivity while reducing liver lipid content. On high-fat diet, JAK2L mice had hepatic steatosis and insulin resistance despite protection from diet-induced obesity. JAK2LA mice had higher liver lipid content and no protection from obesity but retained exquisite hepatic insulin sensitivity. AKT activity was selectively attenuated in JAK2L adipose tissue, whereas hepatic insulin signaling remained intact despite profound hepatic insulin resistance. Therefore, JAK2 in adipose tissue is epistatic to liver with regard to insulin sensitivity and responsiveness, despite fatty liver and obesity. However, hepatocyte autonomous JAK2 signaling regulates liver lipid deposition under conditions of excess dietary fat. This work demonstrates how various tissues integrate JAK2 signals to regulate insulin/glucose and lipid metabolism.

The regulation of glucose metabolism by the anterior pituitary gland was described nearly 100 years ago. Hypophysectomy sensitizes animals to the hypoglycemic effects of insulin, whereas conversely, hypophyseal extracts confer potent diabetogenic activity (1). The major anterior pituitary-derived diabetogenic factor was determined to be growth hormone (GH) (2). However, treatment with recombinant GH has ostensible beneficial effects, such as reductions in fat mass (3), and patients with GH deficiency (GHD) or insensitivity (GHI) may be prone to nonalcoholic steatohepatitis (NASH) and fatty liver (4), complicating the discussion around the potential metabolic benefits of inhibiting GH action.

GH signals through the GH receptor (GHR), JAK2, and then STAT5 to induce *Igf1*. Hepatocyte GH signaling controls levels of circulating IGF-I, which in turn feedback inhibits GH secretion in the hypothalamus/pituitary gland (5). Therefore, when hepatocyte GH signaling is inhibited at the level of the GHR, JAK2, or STAT5, circulating GH levels increase and can hyperstimulate other GH responses, such as adipose tissue lipolysis.

Although GH is unquestionably a potent mediator of adipose tissue lipolysis (6), whether GH modulates lipolysis directly or indirectly remains unknown. We have shown that GH promotes lipolysis indirectly through inhibitory effects on insulin action and that short-term GH administration

[1]Cardiovascular Research Institute, University of California, San Francisco, San Francisco, CA

[2]Department of Internal Medicine, Yale University School of Medicine, New Haven, CT

[3]Division of Endocrinology and Metabolism, Department of Medicine, University of Pittsburgh, Pittsburgh, PA

[4]Cardiovascular and Metabolic Diseases, Pfizer, Cambridge, MA

[5]Department of Cellular and Molecular Physiology, Yale University School of Medicine, New Haven, CT

[6]Howard Hughes Medical Institute, Yale University School of Medicine, New Haven, CT

M.J.J. and E.J.W. are co-senior authors.

Corresponding author: Ethan J. Weiss, ethan.weiss@ucsf.edu.

METABOLISM

induces insulin resistance (6,7). This finding puts forth a mechanistic explanation of the Houssay effect wherein high levels of circulating GH promote adipocyte lipolysis, the by-products of which drive hepatic insulin resistance (8). Data supporting this hypothesis show that inhibition of lipolysis in patients with acromegaly normalizes hepatic insulin sensitivity (9,10). Therefore, adipose tissue regulates many of the biological consequences of GH signaling, including liver metabolism.

Although hepatocyte-specific GHI through deletion of *Ghr* (11), *STAT5* (12), or *Jak2* (5,13) leads to fatty liver, precisely how GH leads liver lipid deposition remains unclear. GH has been shown to be an inhibitor of hepatic de novo lipogenesis (DNL) because induction of hepatocyte-specific, adult-onset GHD increases DNL (14). However, we did not observe differences in DNL in mice with congenital hepatocyte-specific GHI (JAK2L) (6). Furthermore, we have demonstrated that concomitant disruption of hepatocyte *Cd36* largely prevents fatty liver in JAK2L mice, suggesting that hepatic GH signaling–mediated regulation of fatty acid uptake is important in determining liver lipid content (15). Of note, although *Cd36* disruption restored normal liver lipid levels, reversal of the fatty liver phenotype did not restore insulin sensitivity, suggesting that a tissue other than liver likely governs hepatic insulin sensitivity. Consistent with this finding, genetic disruption of GH secretion or concomitant deletion of adipocyte *Jak2* prevents fatty liver development in mice that cannot transduce hepatic GH signals (5,6).

Insulin signaling is transduced through insulin receptor tyrosine kinase engagement and autophosphorylation followed by a kinase cascade centered on AKT, an obligate regulator of insulin-mediated physiology (16). AKT activation is associated with phosphorylation of two key residues, threonine 308 and serine 473, by PDK1 and mTORC2 kinases, respectively (17). Activated AKT then phosphorylates a number of targets, including PRAS40/AKT1S1, an mTORC1 inhibitor and regulator of glucose homeostasis (18). Insulin stimulates phosphorylation of PRAS40 on threonine 246 through AKT, relieving PRAS40-mediated inhibition of mTORC1 (19). The role of cell-autonomous insulin signaling in the regulation of hepatic insulin sensitivity is debated, with some studies favoring a dominant role of insulin action in liver (20) and others finding hepatic insulin signaling to be dispensable (21).

In the current study, we use hyperinsulinemic-euglycemic clamps and targeted lipidomics to describe the respective metabolic roles of liver and adipose JAK2. In chow-fed mice, those with hepatocyte GHI (JAK2L) were insulin resistant, whereas combined hepatocyte-adipocyte GHI (JAK2LA) restored insulin sensitivity. Insulin resistance in JAK2L mice correlated with high levels of fed circulating fatty acids and liver triacylglycerol (TAG) and diacylglycerol (DAG), all of which were reduced dramatically in insulin-sensitive JAK2LA mice. After a high-fat diet (HFD), hepatic insulin sensitivity further deteriorated in JAK2L mice, whereas JAK2LA mice retained exquisite hepatic and whole-body insulin sensitivity despite developing profound fatty liver. Although no defects in insulin-stimulated AKT phosphorylation were observed in

the insulin resistant state, AKT activity, as measured by PRAS40 threonine 246 phosphorylation, was selectively attenuated in JAK2L adipose tissue. Of note, hepatic insulin resistance in JAK2L mice was not associated with reduced liver insulin signaling under clamped conditions. Therefore, adipocyte JAK2 appears to be epistatic to hepatocyte JAK2 with regard to insulin sensitivity and fatty liver in chow-fed animals. However, after HFD, loss of adipocyte *Jak2* is insufficient to prevent fatty liver in mice with hepatocyte GHI. Finally, disruption of JAK2 in adipose tissue is sufficient to maintain remarkable hepatic insulin sensitivity in the face of altered hepatic lipid metabolism.

RESEARCH DESIGN AND METHODS

Animals and Diets
Production of *albumin:CRE;Jak2^lox/lox* (JAK2L) and compound *albumin:CRE;Jak2^lox/lox/adiponectin:CRE;Jak2^lox/lox* (JAK2LA) mice were previously described (6). *Jak2^lox/lox* mice (22) were backcrossed onto the C57BL/6 background for at least nine generations and used as the control (CON). For chow studies, mice were fed PicoLab Mouse Diet 20 (LabDiet #5058; 23% of calories from protein, 22% from fat, and 55% from carbohydrate), and for HFD studies, mice were fed Research Diets D12492 (20% of calories from protein, 60% from fat, and 20% from carbohydrate).

Animal Studies and Sample Collection
Six-week-old CON, JAK2L, and JAK2LA mice were fed an HFD or were maintained on chow for 10 weeks. Total fat mass was determined by DEXA on isoflurane-anesthetized mice by using a Lunar PIXImus2 densitometer (GE Healthcare). Blood glucose and serum insulin levels were determined after a 16-h overnight fast by hand-held glucometer (Bayer) and ELISA (ALPCO), respectively. For insulin tolerance testing (ITT), mice were fasted for 4 h (0900–1300 h) followed by intraperitoneal injection of 1 unit/kg insulin (Novolin; Novo Nordisk, Bagsværd, Denmark). Blood glucose levels were determined by tail prick with a hand-held glucometer at the times indicated. Free fatty acid (FFA) levels were determined by using an enzyme-linked colormetric assay (Wako). For final tissue collection, samples were collected from ad libitum fed mice starting at 1000 h by using standard sterile techniques. Tissue was harvested and immediately snap frozen in liquid nitrogen or suspended in 4% paraformaldehyde for histological analysis. Blood was collected from the retroorbital sinus and allowed to clot before centrifugation at 10,000*g* for 10 min at 4°C for serum separation. Serum was stored at −80°C before analyses. Clinical chemistry was performed by the University of California, Davis, Comparative Pathology Laboratory.

Hyperinsulinemic-Euglycemic Clamp Studies
Clamp studies were performed according to recommendations of the National Institutes of Health–funded Mouse Metabolic Phenotyping Consortium and as previously described (23,24). Briefly, mice recovered 1 week after receiving surgery to implant an indwelling jugular vein catheter before clamp

studies. Mice were fasted overnight and received a basal infusion of 3-^{3}H-glucose conjugated to BSA to determine fasting glucose. A primed/continuous infusion of insulin and 3-^{3}H-glucose was administered alongside a variable infusion of 20% dextrose to maintain euglycemia during the hyperinsulinemic portion of the study. A 10-μCi bolus injection of ^{14}C-2-deoxyglucose was given at 90 min to determine tissue-specific glucose uptake, which was calculated from the area under the curve of ^{14}C-2-deoxyglucose detected in plasma and the tissue content of ^{14}C-2-deoxyglucose-6-phosphate. Blood was collected by tail massage at set intervals, and glucose levels were measured by glucose oxidase method. Insulin infusion rates were as follows: chow 2.5 mU · kg^{-1} · min^{-1} and HFD 4.0 mU · kg^{-1} · min^{-1}. Glucose turnover was determined as the ratio of the 3-^{3}H-glucose infusion rates (GIRs) to the specific activity corrected to the contribution of the infusion rate during the last 40 min of the hyperinsulinemic infusion. Calculation of endogenous glucose production (EGP) and tissue-specific glucose uptake were described previously (24). For chow studies, mice were ~16 weeks of age, and HFD study mice were age-matched to chow study mice and fed an HFD for 4 weeks before clamps.

Lipidomics
Liver lipidomics and total hepatic triglyceride (TG) analyses were carried out exactly as previously described (15).

Quantitative PCR
Quantitative PCR and analysis for liver Cd36 was performed exactly as previously described (15).

Western Blots
Liver, gastrocnemius, and epididymal adipose depots were excised from HFD-fed mice at the end of hyperinsulinemic-euglycemic clamps and flash frozen. Tissues were homogenized in a precooled bead mill (Retsch MM400) in radioimmuno-precipitation assay buffer (50 mmol/L Tris, 150 mmol/L NaCl, 1% Triton X-100, 0.5% sodium deoxycholate, 0.1% SDS, pH 8.0) with Halt Protease and Phosphatase Inhibitor Cocktail (78440; Thermo Fisher Scientific) for 2 min at 30 oscillations/s. Samples were placed on a tube rotator for 30 min at 4°C and then centrifuged at 10,000g for 10 min to remove the nuclear pellet. Immunoblots were performed with 10 μg total protein on 15-well, 4–12% Bolt Bis-Tris Plus Gels (Thermo Fisher Scientific). Membranes were stained with REVERT Total Protein Stain (LiCor) for normalization purposes and incubated overnight with antibodies from Cell Signaling Technology: pan-AKT (#2920), pSer473-AKT (#4060), PRAS40 (#2610), and pThr246-PRAS40 (#2997). Digital images were quantified by using LiCor Image Studio version 5.2 for Western blot analysis. Each individual membrane was normalized to the REVERT Total Protein Stain, and the ratio of phosphorylated to total protein was calculated.

Study Approval
All animal studies were approved by institutional animal care and use committees at the University of California, San Francisco; University of Pittsburgh; and Yale University.

Statistics and Graphics
All statistical tests and figures were performed with GraphPad Prism version 6.0 software.

RESULTS

Adipocyte JAK2 Signaling Mediates Insulin Sensitivity in Mice With Hepatocyte-Specific GHI
Chow-fed JAK2L and JAK2LA mice weighed less than CON mice (Fig. 1A), whereas JAK2LA mice had increased total fat mass (Fig. 1B) and percent fat mass as per total body weight versus CON and JAK2L mice (Fig. 1C). Therefore, concomitant loss of adipocyte Jak2 on the JAK2L background, similar to adipocyte-only Jak2 deletion (7), promoted adiposity. The increased fat mass occurred in both visceral (Fig. 1D) and subcutaneous (Fig. 1E) depots. Fed JAK2L mice had increased plasma FFAs that were reduced by concomitant deletion of adipocyte Jak2 (Fig. 1F). There was both fasting hyperglycemia (Fig. 1G) and hyperinsulinemia (Fig. 1H) in JAK2L mice that, as with fed FFA levels, were normalized in JAK2LA animals. Thus, JAK2L mice have insulin resistance that is normalized by disruption of adipocyte Jak2. Indeed, ITTs revealed overt insulin resistance in JAK2L mice, whereas JAK2LA mice were identical to CON mice.

Chow-Fed JAK2L Mice Have Profound Hepatic and Whole-Body Insulin Resistance, Which Are Normalized in JAK2LA Mice
To definitively determine tissue-specific insulin sensitivity, hyperinsulinemic-euglycemic clamps were performed. No difference in clamped plasma insulin levels were found between the groups during the experiment (Supplementary Fig. 1A), and plasma glucose levels were matched during steady-state or the last 40 min of the clamp at ~120 mg/dL (Fig. 2A). Compared to controls, JAK2L mice required a lower GIR to maintain euglycemia, whereas the JAK2LA cohort did not differ from CON mice (Fig. 2B and C), confirming normalization of whole-body insulin sensitivity. Consistent with fasting hyperglycemia (Fig. 1G), basal EGP was increased in JAK2L animals (Fig. 2D). Furthermore, clamped JAK2L mice were completely resistant to insulin-mediated reductions in EGP (Fig. 2E and F), demonstrating profound hepatic insulin resistance. Hepatic insulin sensitivity was restored to CON levels in JAK2LA mice (Fig. 2E and F). Whole-body glucose disposal was reduced in JAK2L but not JAK2LA mice (Fig. 2G). Skeletal muscle glucose uptake did not differ statistically by genotype (Fig. 2H), whereas adipose tissue glucose uptake was reduced in both JAK2L and JAK2LA animals (Fig. 2I). Therefore, disruption of adipocyte Jak2 normalizes whole-body and hepatic insulin sensitivity in mice with hepatocyte-specific GHI.

Reductions in adipocyte lipolysis and plasma FFA have been shown to be major regulators of insulin-mediated suppression of hepatic glucose output (8). Therefore, we measured plasma FFA levels in awake and unanesthetized clamped CON, JAK2L, and JAK2LA mice. Overnight fasted, basal FFA levels were reduced in JAK2LA plasma (Fig. 2J).
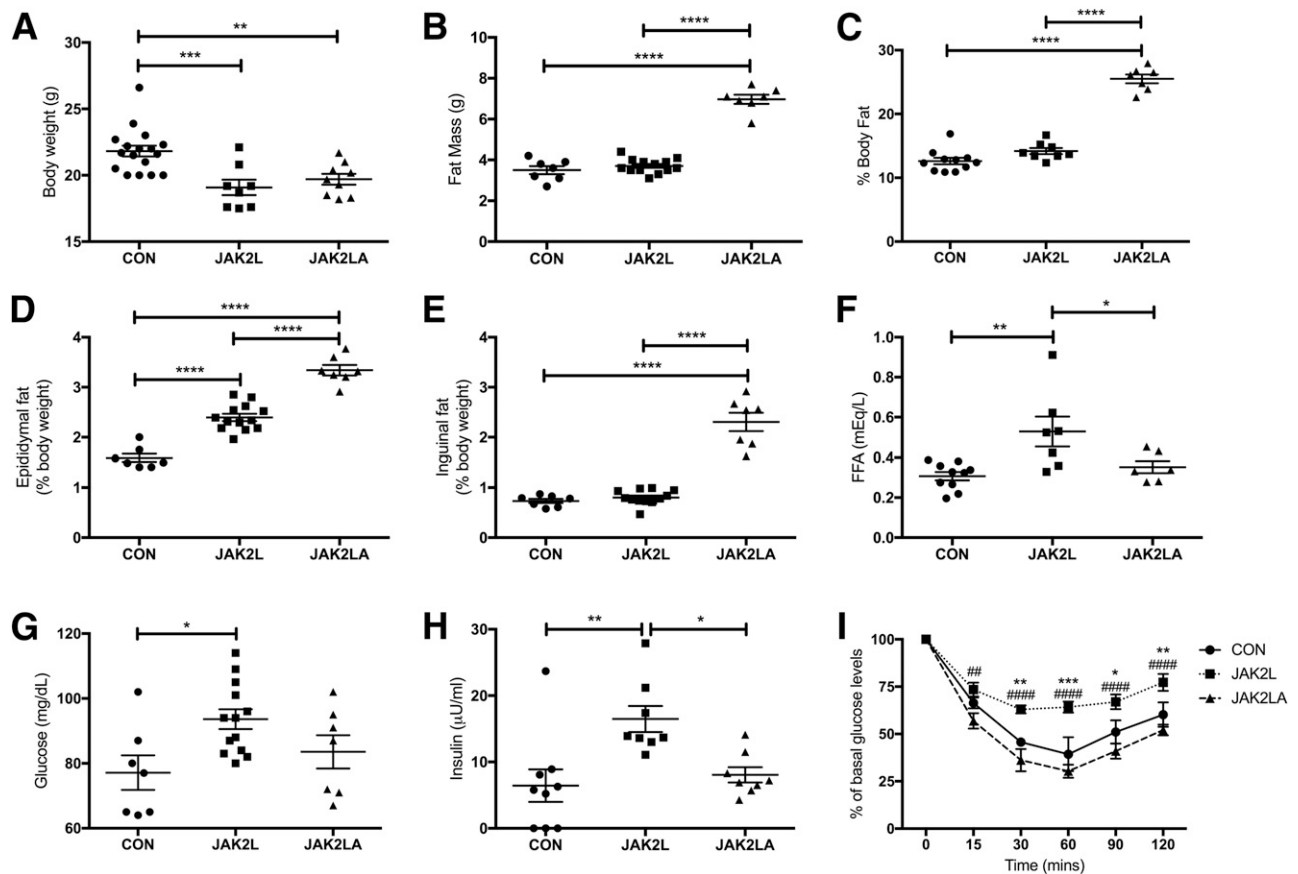
Figure 1—Loss of adipocyte *Jak2* normalizes insulin responsiveness in chow-fed mice lacking hepatocyte *Jak2*. *A* and *B*: Total body weight and fat mass in CON, JAK2L, and JAK2LA mice. *C*: Percent body fat as a fraction of total body weight. *D* and *E*: Percent epididymal visceral and inguinal subcutaneous fat as a fraction of total body weight. *F*: Fed plasma FFAs. *G* and *H*: Fasting blood glucose and plasma insulin. *I*: ITT expressed as a percentage of basal (fasting) glucose in CON, JAK2L, and JAK2LA mice. n = 7–19 mice/cohort. Data are mean ± SEM. *$P <$ 0.05, **$P <$ 0.01, ***$P <$ 0.001, ****$P <$ 0.0001 (for CON vs. JAK2L in *I*); ##$P <$ 0.01, ####$P <$ 0.0001 (for JAK2L vs. JAK2LA in *I*) by one-way (*A–H*) or two-way (*I*) ANOVA.

After insulin infusion, plasma FFA in CON mice was suppressed by ~60%, whereas FFA levels were reduced by ~25% in JAK2L and JAK2LA mice (Fig. 2*K* and *L*). Therefore, although the impaired suppression of lipolysis in the JAK2L mice and concomitant hepatic insulin resistance was consistent with a regulatory role of lipolysis on hepatic glucose production, this effect was not apparent in JAK2LA mice. In addition, differences in absolute levels of plasma FFA levels did not correlate with hepatic insulin sensitivity in clamped JAK2L and JAK2LA mice.

Adipocyte *Jak2* Governs Hepatic Lipid Content in Chow-Fed JAK2L Mice

We previously determined that JAK2L mice develop fatty liver on a chow diet, and this is improved in compound JAK2LA animals (6). To determine the hepatic lipid composition in these groups, we performed comprehensive targeted liver lipidomics. Most TAG (Fig. 3*A*) and DAG (Fig. 3*B*) species were elevated in JAK2L livers compared with CON, and these were partially restored in JAK2LA livers. Total hepatic cholesterol ester (CE) levels did not differ among the groups, although a clear shift was observed away from longer-chain,

unsaturated CE in JAK2L and JAK2LA livers (Fig. 3*C*). Most species of hepatic ceramide (CER) levels were increased in JAK2LA versus CON and JAK2L mice (Fig. 3*D*). These data support a potential role for reductions in hepatic TAG and DAG content in mediating the normalized hepatic insulin sensitivity seen in JAK2LA mice.

JAK2LA Mice Maintain Exquisite Hepatic Insulin Sensitivity After HFD

The results from the normal chow-fed cohort strongly suggest that the profound whole-body and hepatic insulin resistance observed in JAK2L mice depended on the marked increase in liver lipid content. To explore this further, we next challenged mice with an HFD. JAK2L mice were resistant to HFD-induced obesity (Supplementary Fig. 1*B*), whereas no difference was found in body weight or adiposity between CON and JAK2LA mice (Fig. 4*A–C*). JAK2L animals had reduced visceral (Fig. 4*D*) and subcutaneous (Fig. 4*E*) adipose mass (vs. CON), whereas a selective expansion of the inguinal subcutaneous depot was observed in JAK2LA animals versus CON (Fig. 4*D* and *E*). Ad libitum fed FFA levels did not differ by genotype in HFD-fed mice (Fig. 4*F*). As seen in
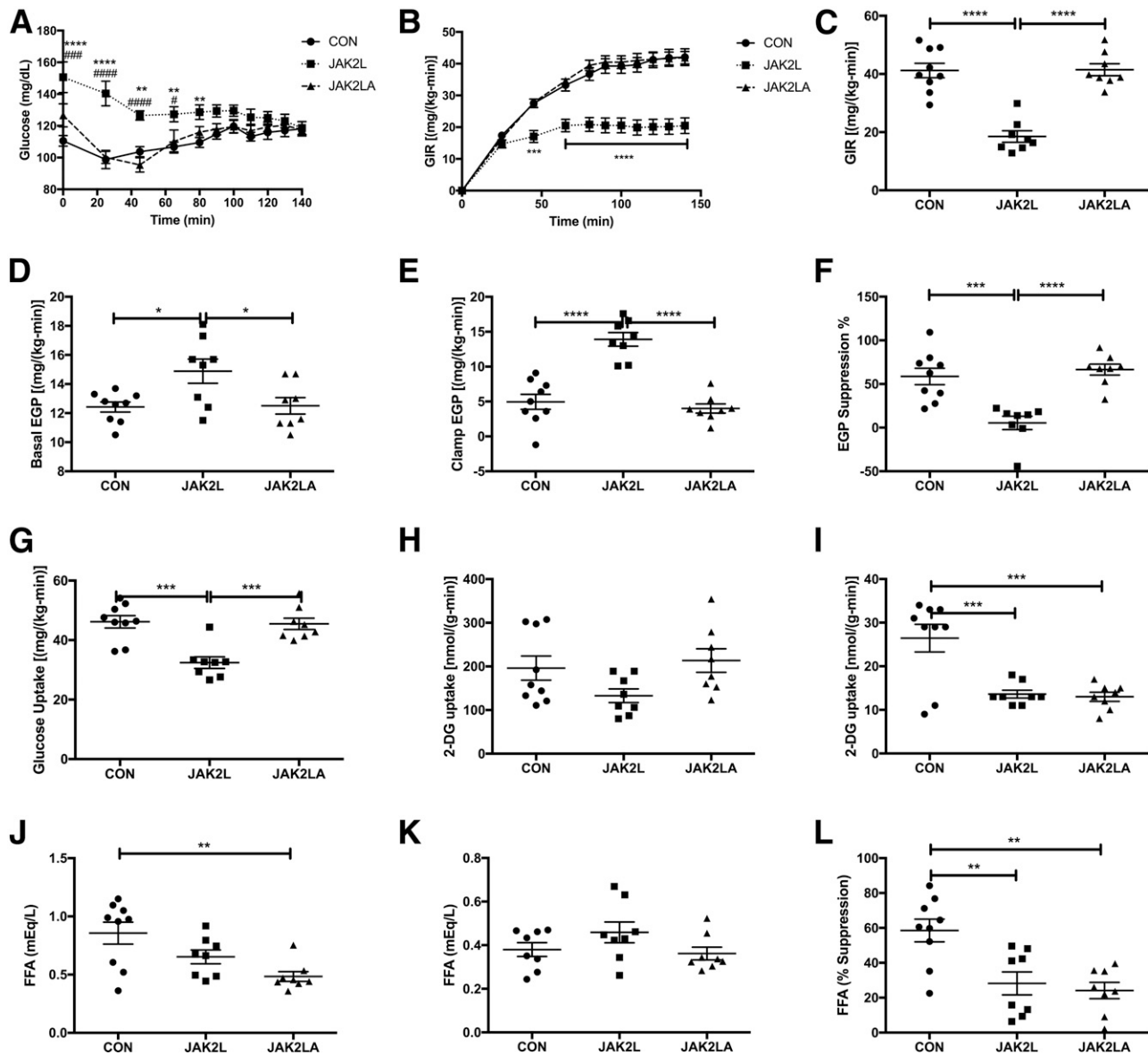
Figure 2—Loss of hepatocyte *Jak2* induces hepatic insulin resistance in chow-fed mice in an adipocyte *Jak2*–dependent manner. *A* and *B*: Blood glucose levels and GIR during glucose infusion to achieve euglycemia in CON, JAK2L, and JAK2LA mice. *C*: GIR at euglycemia. *D* and *E*: Basal and clamped EGP. *F*: Percent suppression of EGP after insulin infusion. *G*: Whole-body glucose uptake. *H* and *I*: Tissue-specific glucose uptake in gastrocnemius and epididymal visceral fat. *J* and *K*: Basal and clamped plasma FFA levels. *L*: Percent suppression of plasma FFA after insulin infusion. $n = 8$–9 mice/cohort. Data are mean ± SEM. *A*: **$P < 0.01$, ****$P < 0.0001$ (CON vs. JAK2L) and #$P < 0.5$, ###$P < 0.001$, ####$P < 0.0001$ (JAK2L vs. JAK2LA) by two-way ANOVA. *B*: ***$P < 0.001$, ****$P < 0.0001$ for both CON vs. JAK2L and JAK2L vs. JAK2LA by two-way ANOVA. *C–L*: *$P < 0.05$, **$P < 0.01$, ***$P < 0.001$, **** $P < 0.0001$ by one-way ANOVA. 2-DG, 2-deoxy-D-glucose.

the chow-fed cohort, JAK2L mice were hyperglycemic (Fig. 4G) and hyperinsulinemic versus CON mice (Fig. 4H). Despite having similar fasting glucose levels, JAK2LA mice were hypoinsulinemic compared with CON mice (Fig. 4H). Consistent with this finding, JAK2LA mice were hyperresponsive to insulin during ITT (Fig. 4I).

HFD-Fed JAK2LA Mice Retain Hepatic Insulin Sensitivity
We next performed hyperinsulinemic-euglycemic clamps to definitively determine tissue-specific insulin sensitivity in the HFD-challenged mice. Plasma insulin (Supplementary

Fig. 1C) and glucose levels (Fig. 5A) were matched during steady state in response to a fixed- and variable-rate infusion of each, respectively, during the clamp. At steady-state euglycemia, the GIR in JAK2LA mice was 222% greater than CON levels (Fig. 5B and C). Conversely, JAK2L mice required ~65% lower GIR than CON mice. Although basal EGP did not statistically differ among groups (Fig. 5D), no suppression of EGP occurred after insulin infusion in JAK2L mice (Fig. 5E and F). On the other hand, insulin fully suppressed EGP in clamped JAK2LA animals, and this was statistically greater than in both JAK2L
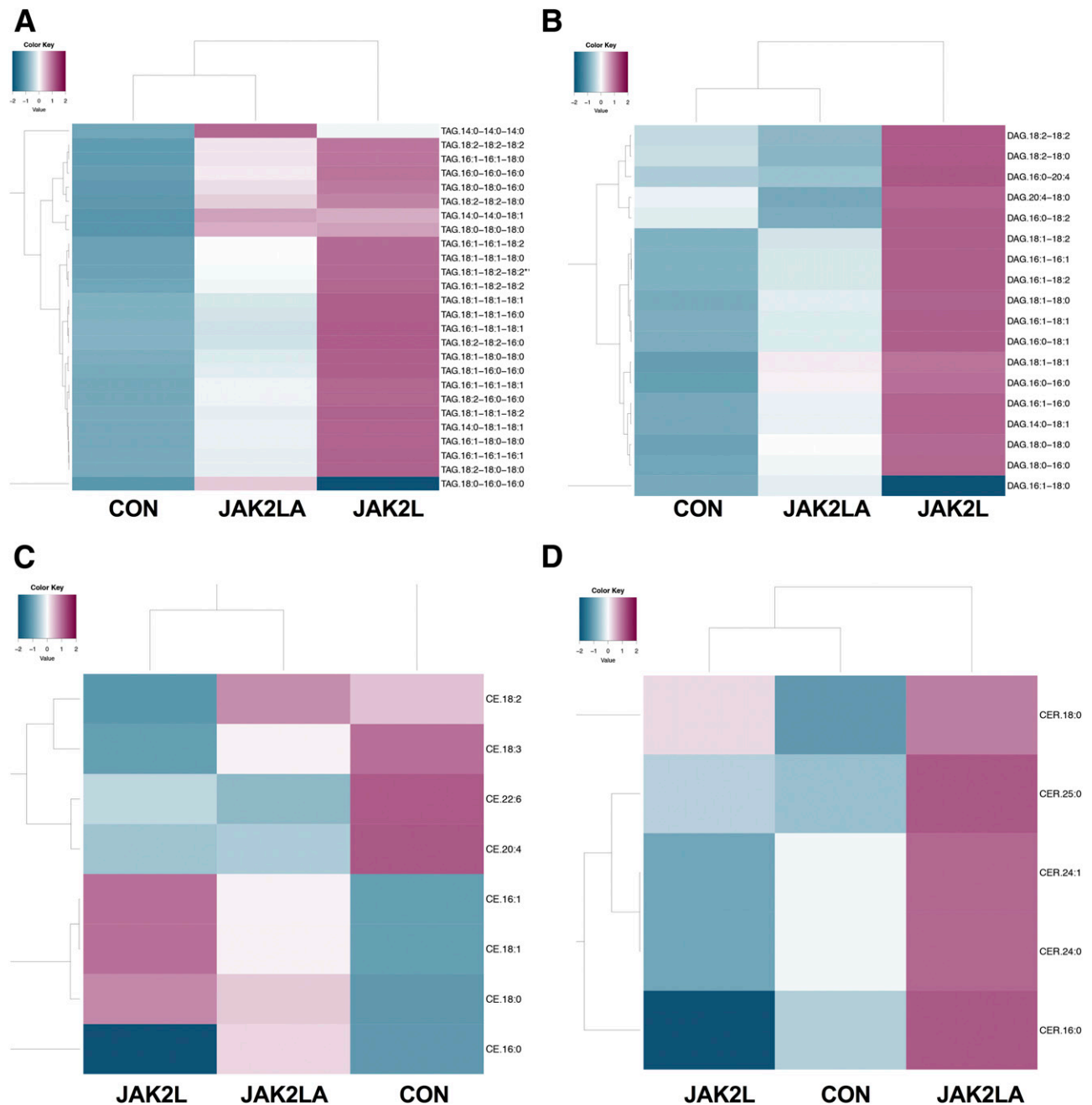
Figure 3—Hepatic lipids in chow-fed mice. Heat map and hierarchical clustering of lipidomics results from the livers of chow-fed CON, JAK2L, and JAK2LA mice showing TAG species (A), DAG species (B), CE species (C), and CER species (D). $n = 5$/cohort.

and CON mice (Fig. 5E and F). Whole-body glucose disposal (Fig. 5G) as well as skeletal muscle (Fig. 5H) and adipose tissue glucose uptake (Fig. 5I) were increased in JAK2LA mice. Neither whole-body glucose disposal (Fig. 5G) nor skeletal muscle glucose uptake (Fig. 5H) differed between CON and JAK2L mice, whereas adipose tissue glucose uptake was reduced in JAK2L mice (Fig. 5I). Therefore, loss of hepatocyte Jak2 abrogates insulin sensitivity almost entirely through inhibition of insulin-mediated suppression of EGP. Concomitant disruption of adipocyte Jak2 confers protection from whole-body and

hepatic insulin resistance compared with CON and JAK2L mice.

As opposed to effects on basal EGP, overnight fasted, basal FFA levels in HFD-fed JAK2LA mice were decreased (Fig. 5J). After insulin infusion, plasma FFA levels (Fig. 5K) were suppressed by ~46%, 27%, and 52% in the CON, JAK2L, and JAK2LA mice, respectively, although these disparities were not significant (Fig. 5L). In contrast to chow data where there were no differences in plasma FFA levels under clamped conditions (Fig. 2K), plasma FFA levels were markedly lower in JAK2LA mice than in CON and JAK2L
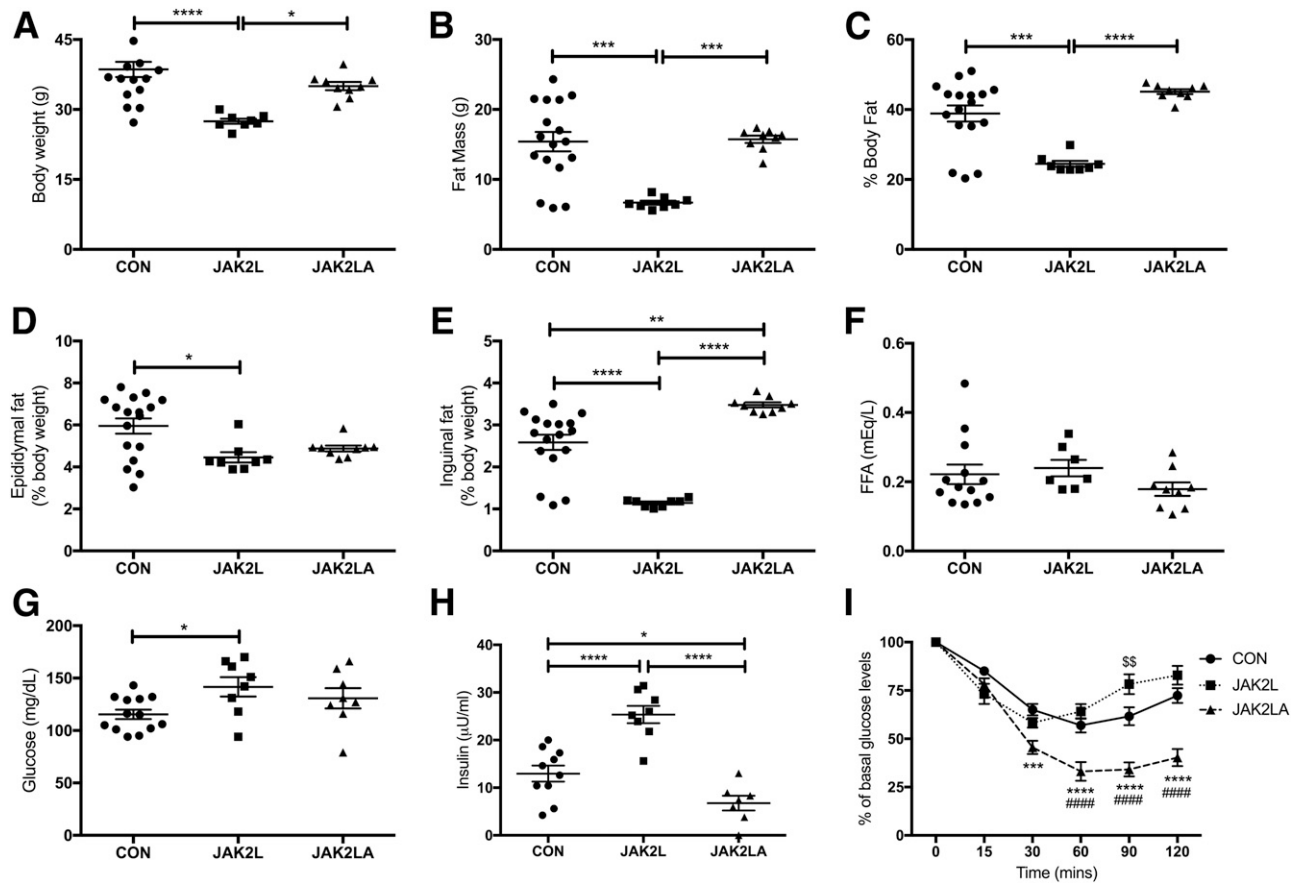
Figure 4—JAK2LA mice maintain exquisite insulin responsiveness after dietary challenge. A and B: Total body weight and fat mass in CON, JAK2L, and JAK2LA HFD-fed mice. C: Percent body fat as a fraction of total body weight. D and E: Percent epididymal visceral and inguinal subcutaneous fat as a fraction of total body weight. F: Fed plasma FFAs. G and H: Fasting blood glucose and plasma insulin. I: ITT expressed as a percentage of basal (fasting) glucose in CON, JAK2L, and JAK2LA mice. $n = 7–17$/cohort. Data are mean $\pm$ SEM. *$P < 0.05$, **$P < 0.01$, ***$P < 0.001$, ****$P < 0.0001$ (for CON vs. JAK2LA in I); ####$P < 0.0001$ (for JAK2L vs. JAK2LA in I); $$$$P < 0.01$ (for CON vs. JAK2L in I) by one-way (A–H) or two-way (I) ANOVA.

mice, which were not different (Fig. 5K). Therefore, although reduced plasma FFAs and improved hepatic insulin sensitivity in HFD-fed JAK2LA mice were consistent with the concept that lipolysis regulates hepatic glucose production, the lack of difference in plasma FFAs between CON and JAK2L mice despite clear differences in clamped rates of hepatic glucose production did not (Fig. 5E and K). As in chow-fed mice, differences in circulating FFA levels did not correlate with divergences in hepatic insulin sensitivity.

Loss of Adipocyte JAK2 Confers Hepatic Insulin Sensitivity in the Face of Fatty Liver

After HFD, total hepatic TAG (Fig. 6A), CE (Fig. 6C), and CER (Fig. 6D) levels were highest in the JAK2LA cohort. Total DAG levels were highest in JAK2L liver, with levels in JAK2LA liver intermediate to CON liver. However, individual species also were elevated in JAK2LA versus CON liver (Fig. 6B). Therefore, although loss of adipocyte Jak2 is epistatic to liver JAK2 in terms of hepatic insulin sensitivity, compound adipocyte-hepatocyte Jak2 deletion did not prevent HFD-induced fatty liver.

Loss of Hepatocyte Jak2 Induces Hepatic Insulin Resistance Independent of Altered Liver Insulin Signaling

To determine how hepatic insulin resistance occurs in an adipocyte Jak2–dependent manner, we assessed signaling in insulin-responsive tissues of HFD-fed mice at the end of hyperinsulinemic-euglycemic clamps. Despite profound physiological hepatic insulin resistance, levels of neither phosphorylated (serine 473, pAKT) AKT nor phosphorylated PRAS40 (threonine 246, pPRAS40) were attenuated in livers of clamped JAK2L mice (Fig. 7A–C). To determine whether livers of clamped mice were exposed to sufficient insulin to adequately assess hepatic insulin signaling, we compared pAKT in the fasted (basal) state with that of clamped tissue. Although levels of pAKT were increased on average by >300%, these results were not significant (Supplementary Fig. 2). Basal levels of pAKT were higher in JAK2L and JAK2LA livers, and no induction with insulin (clamped samples) was found. Therefore, we cannot exclude the possibility that our clamp studies might preferentially highlight the indirect (e.g., adipocyte) effects of hepatic insulin
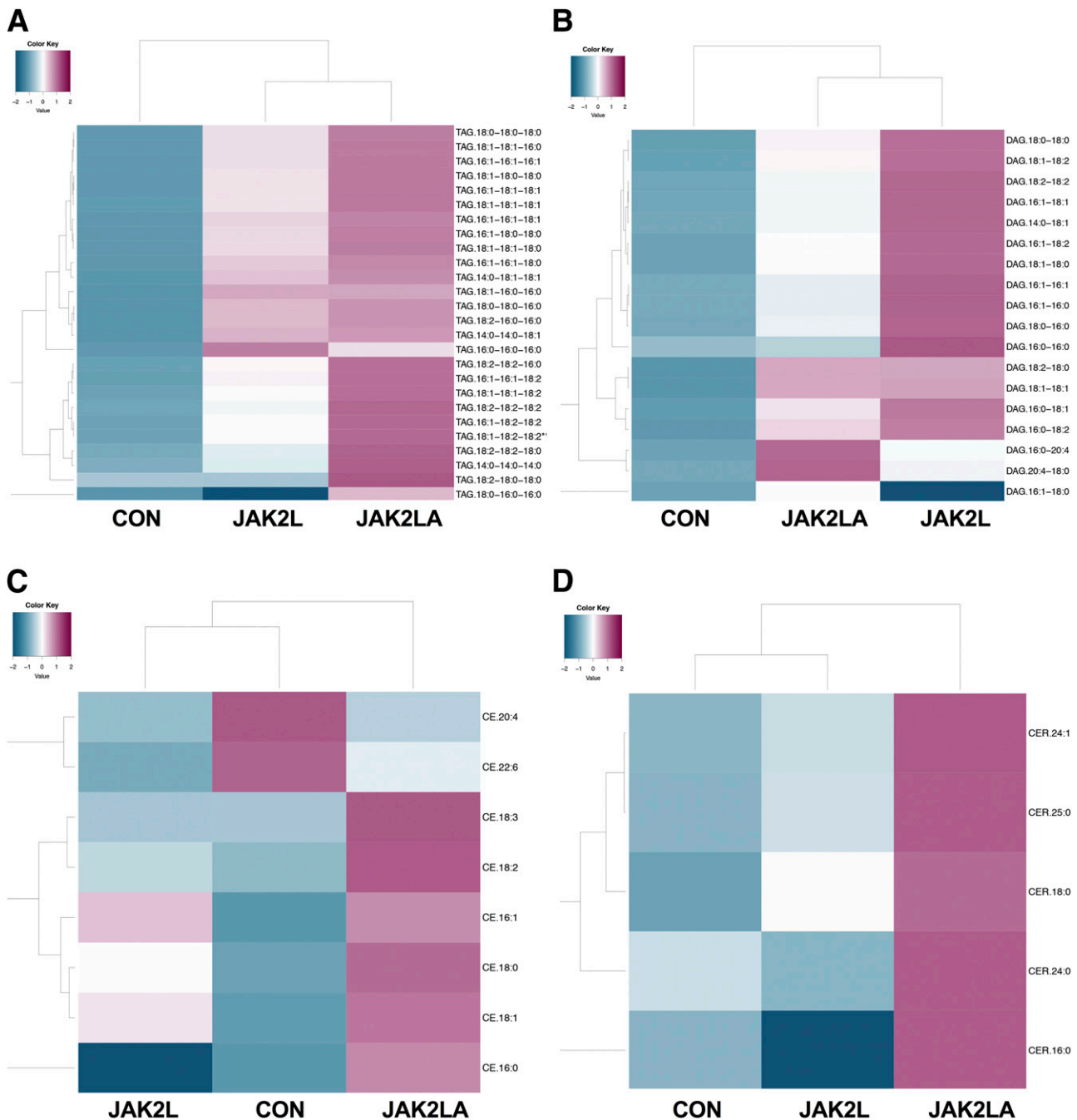
Figure 5—Loss of adipocyte *Jak2* imparts hepatic and whole-body insulin sensitivity in HFD-fed mice on the JAK2L background. *A* and *B*: Blood glucose levels and GIR during glucose infusion to achieve euglycemia in CON, JAK2L, and JAK2LA mice. *C*: GIR at euglycemia. *D* and *E*: Basal and clamped EGP. *F*: Percent suppression of EGP after insulin infusion. *G*: Whole-body glucose uptake. *H* and *I*: Tissue-specific glucose uptake in gastrocnemius and epididymal visceral fat. *J* and *K*: Basal and clamped plasma FFA levels. *L*: Percent suppression of plasma FFA after insulin infusion. $n = 6$–10/cohort. Data are mean ± SEM. *$P < 0.05$, **$P < 0.01$, ***$P < 0.001$, ****$P < 0.0001$ (for CON vs. JAK2LA in *A* and *B*); #$P < 0.05$, ##$P < 0.01$, ####$P < 0.0001$ (for JAK2L vs. JAK2LA in *A* and *B*); \$$P < 0.05$ (for CON vs. JAK2L in *A*) by two-way (*A* and *B*) or one-way (*C*–*L*) ANOVA.

sensitivity regulation. In other insulin sensitive tissues, such as skeletal muscle and epididymal adipose tissue (Fig. 7*D*–*F*), pAKT and pPRAS40 were augmented in JAK2LA mice, consistent with the glucose uptake data from HFD-fed clamped mice (Fig. 5*H* and *I*). Of note, adipose tissue pAKT levels were attenuated in mice lacking hepatocyte Jak2, and this was entirely reversed by concomitant deletion of adipocyte *Jak2* (Fig. 7*G*–*I*). Therefore, insulin resistance in JAK2L mice is associated with disruption of adipose tissue insulin signaling in an adipocyte JAK2–dependent manner.

JAK2LA Mice Uncouple Liver Fat and Adiposity From Insulin Sensitivity

Given the strong positive correlations between steatosis and adiposity with insulin resistance, we examined these parameters against whole-body and hepatic insulin sensitivity in JAK2L and JAK2LA mice. As expected, whole-body insulin sensitivity, as measured by GIR, fell precipitously when CON mice were fed HFD, which was associated with increased liver TGs (Fig. 8*A*) and percent body fat (Fig. 8*B*). The same trend was observed for JAK2L mice. Conversely, increased liver TG and body fat after HFD were coincident with augmented

Figure 6—JAK2LA mice develop fatty liver after an HFD. Heat map and hierarchical clustering of lipidomics results from livers of HFD-fed CON, JAK2L, and JAK2LA mice showing TAG species (A), DAG species (B), CE species (C), and CER species (D). n = 5/cohort.

insulin sensitivity in JAK2LA animals. Similar patterns were observed for hepatic insulin sensitivity such that attenuated EGP in CON and JAK2L mice was concurrent with increased hepatic lipid content (Fig. 8C) and adiposity (Fig. 8D). As opposed to these anticipated associations seen in these cohorts, steatosis and increased body fat were associated with augmented hepatic insulin sensitivity in JAK2LA animals. Therefore, JAK2LA mice uncouple the prevalent correlations of hepatic lipid content and adiposity from insulin resistance.

We previously showed that JAK2LA mice have impaired lipolysis, which negatively correlates with insulin sensitivity (6). Therefore, we reasoned that insulin-mediated suppression of circulating FFA, a surrogate marker of lipolysis, would correlate with EGP. In chow-fed CON mice, EGP was reduced ~60% after the clamp, whereas insulin-mediated suppression of FFA was also reduced ~60% (Supplementary Fig. 3A). The near-complete hepatic insulin resistance in clamped JAK2L mice was associated with an ~50% reduction in the ability of insulin to reduce circulating
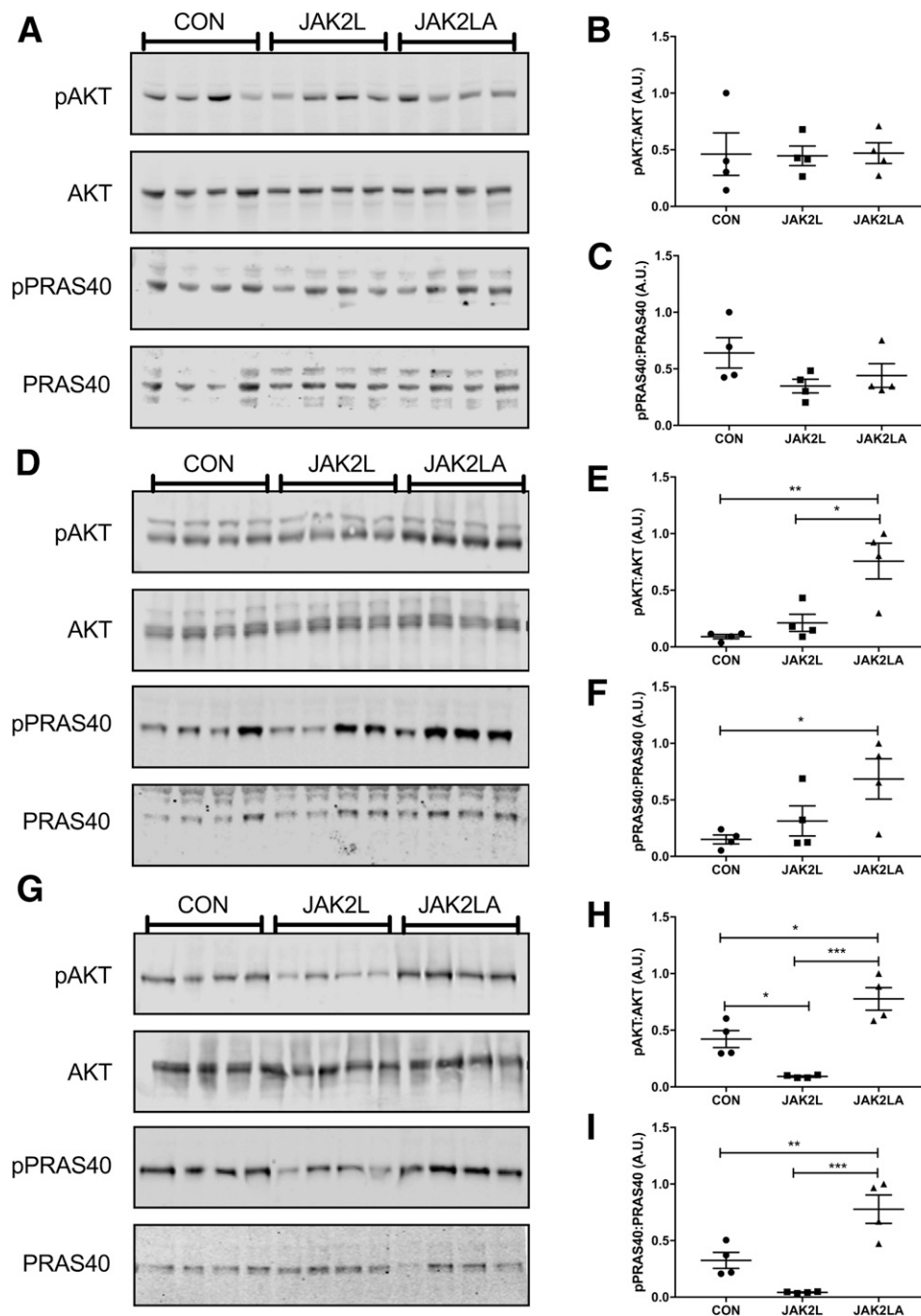
Figure 7—JAK2L mice have normal liver insulin signaling despite hepatic insulin resistance. Liver (*A–C*), gastrocnemius (*D–F*), and epididymal (*G–I*) adipose tissues were collected at the end of the clamp from CON, JAK2L, and JAK2LA HFD-fed mice (Fig. 5). Tissues were lysed and analyzed for phosphorylated AKT (pAKT) and PRAS40 (pPRAS40) as well as for total AKT and PRAS40 by Western blot. Fluorescent LiCor images were used to quantify phosphorylated:total protein ratios. *n* = 4/cohort. Data are mean ± SEM. *$P < 0.05$, **$P < 0.01$, ***$P < 0.001$ by one-way ANOVA. A.U., arbitrary unit.

FFA, consistent with a role for FFA in insulin resistance. However, the maintenance of insulin sensitivity in clamped, chow-fed JAK2LA mice was associated with a reduction in insulin-mediated suppression of plasma FFA (CON 56%, JAK2LA 25%). A similar pattern was noted for HFD-fed mice (Supplementary Fig. 3*B*) such that augmented hepatic insulin sensitivity in clamped JAK2LA mice was not associated with an increase in insulin-mediated reductions in circulating FFA (CON 54%, JAK2LA 55%). Therefore, augmented insulin sensitivity in JAK2LA mice is dissociated from fatty liver, adiposity, and insulin-mediated suppression of lipolysis.
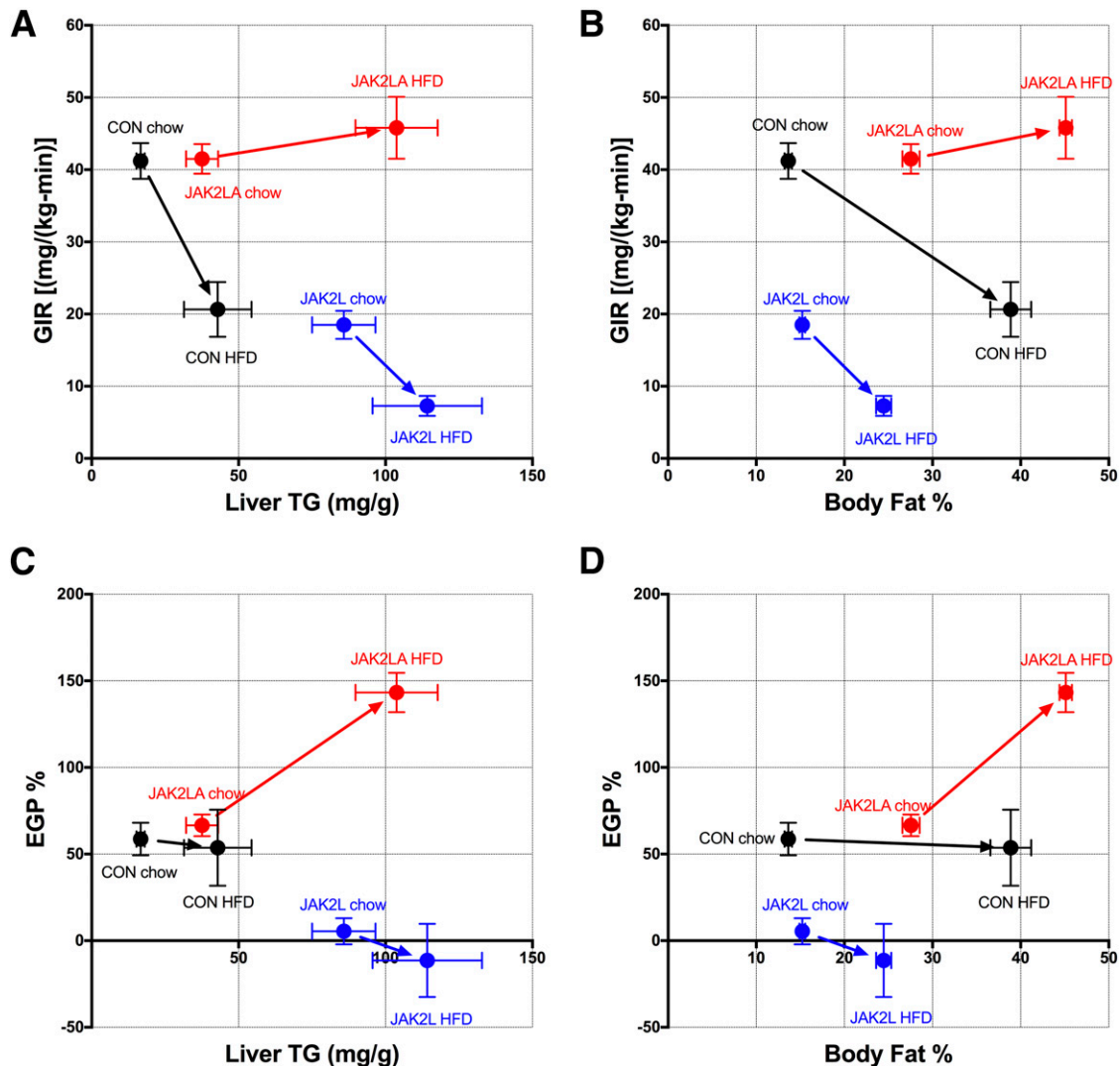
Figure 8—JAK2LA mice uncouple fatty liver and adiposity from insulin resistance. GIR at the end of the clamp plotted against total liver TGs (*A*) and percent body fat (*B*) for CON, JAK2L, and JAK2LA mice fed chow or HFD. Percent suppression of EGP at the end of the clamp plotted against total liver TGs (*C*) and percent body fat (*D*). Plotted are the GIR and EGP at the end of the clamp experiments reported in Figs. 2 (chow) and 5 (HFD), and the means of percent body fat determined from experiments reported in Figs. 1 (chow) and 4 (HFD). Total liver TGs were determined from livers collected from mice used for experiments 1 (chow) and 4 (HFD). $n = 5$–8/cohort. Data are mean $\pm$ SEM.

DISCUSSION

Excess GH has been proposed to be both a cause and a potential treatment for systemic metabolic disease (25). Recombinant GH has ostensible metabolic benefits and has been put forward as a treatment option for diabetes (26). Also confusing the matter around the potential effects of targeting GH for metabolic disease is the vast array of phenotypes associated with loss-of-function GH signaling. In particular, although congenital GHI reduces the lifelong risk of developing diabetes (27), adult-onset GHD is characterized by insulin resistance (28). The mechanisms that drive these disparate findings are unknown. We present data demonstrating that JAK2, an obligate transducer of GH and other cytokine signals, regulates metabolic homeostasis in a tissue-specific manner. Specifically, hepatocyte-specific *Jak2* disruption promotes hepatic and whole-body insulin resistance,

hepatic lipid deposition, resistance to diet-induced obesity, and attenuation of adipose tissue AKT activity. Concomitant loss of adipocyte JAK2 reverses these phenotypes on chow diet. Therefore, adipocyte *Jak2* is epistatic to hepatocyte *Jak2* under chow-fed conditions. However, when challenged with excess dietary lipid, loss of adipocyte JAK2 is unable to overcome the hepatocyte-autonomous effects and resultant hepatic lipid deposition and fails to prevent diet-induced obesity. Regardless, deleting adipocyte *Jak2* is sufficient to maintain and augment insulin sensitivity, even in the face of fatty liver. Of note, however, disrupting adipocyte *Jak2* is sufficient to maintain and augment insulin sensitivity, even in the face of fatty liver and adiposity.

Previously, we showed that net in vivo lipolysis was increased in JAK2L mice and decreased in JAK2LA mice (6). Furthermore, systemic GH treatment indirectly promotes

lipolysis by inhibiting insulin-mediated suppression of lipolysis in an adipocyte *Jak2*–dependent manner (7). Consistent with these data, the current findings did not reveal the same magnitude in reductions in plasma FFA in clamped JAK2L mice compared with CON mice. However, increased hepatic insulin sensitivity in JAK2LA mice did not correlate with augmented insulin-mediated suppression of FFA (Supplementary Fig. 3). Given that circulating FFA levels reflect the balance of tissue release and uptake, the reduced levels of fasting plasma FFA in hyperinsulinemic-euglycemic clamped JAK2L and JAK2LA mice may reflect increased hepatic uptake. Consistent with the finding that GH signaling suppresses hepatocyte *Cd36* expression (15), we found that JAK2LA livers have ~20-fold increased levels of *Cd36* (Supplementary Fig. 1*D*). We previously showed that either hepatic deletion of *Cd36* or loss of adipocyte *Jak2* prevents fatty liver development in chow-fed JAK2L mice (6,15). Collectively, the data support a mechanism whereby hepatocyte-specific GHI drives increased secretion of GH, which in turn induces adipocyte pathway hyperactivation and attenuation of insulin-mediated inhibition of lipolysis. Subsequently, circulating byproducts of adipocyte lipolysis are taken up by hepatocytes in a CD36-dependent manner and promote lipid deposition.

The role of hepatocyte-autonomous insulin signaling in suppressing hepatic glucose output is not clear. Historically, whether insulin-mediated hepatic insulin sensitivity is controlled directly in hepatocytes, indirectly in peripheral tissues, or both has been debated. Elegant experiments from the 1950s to 1990s showed that insulin-mediated suppression of hepatic glucose output is likely controlled by peripheral (indirect) as much as direct hepatic insulin signaling (29). With the publication of the liver insulin receptor knockout mouse, opinion shifted toward the notion that the predominant regulation of hepatic glucose output was through direct insulin signaling in the hepatocyte (30). More recently, clamp studies seemed to indicate that insulin acts directly on the liver to suppress hepatic glucose production (20). However, genetic studies also have shown that hepatic insulin signaling is dispensable for suppression of EGP (21). The extrahepatic mechanism responsible for hepatic insulin sensitivity has been proposed to be adipose tissue lipolysis (8,31). This is consistent with the current recent findings demonstrating that adipose tissue mediates GH-induced hepatic insulin resistance, which correlates with reductions in lipolysis (7). Furthermore, inhibition of lipolysis in GH-treated humans restores insulin sensitivity (9,10). The current experiments support the existence of an extrahepatic mechanism in the regulation of hepatic glucose production. In addition, a defect in AKT activation exists in the adipose tissue of JAK2L mice that is corrected by concomitant disruption of adipocyte *Jak2*, which correlates with augmented physiological hepatic insulin sensitivity.

The current results also demonstrate that chronic adipose tissue exposure to elevated GH, as occurs in JAK2L animals, can interfere with insulin responsiveness at the level of AKT activation. Phosphorylation of PRAS40 threonine 246 by activated AKT relieves the ability of PRAS40 to inhibit mTORC1 (19). Given the reduced levels of adipose tissue phosphorylation of PRAS40 threonine 246 in JAK2L mice, mTORC1 activity may be attenuated. Of note, adipocyte mTORC1 mediates adiposity, hepatic lipid deposition, and systemic insulin sensitivity (32) similar to adipocyte *Jak2* (7). It will be paramount to determine whether mTORC1 is involved in GH-mediated adipocyte physiology.

Insulin sensitivity negatively correlates with hepatic and whole-body lipid content (33,34). However, as we observed here, steatosis and adiposity have been dissociated from insulin resistance (27,35,36). The mechanism behind the uncoupling of insulin resistance from hepatic lipid accumulation is unknown. Examples exist of nonalcoholic fatty liver disease (NAFLD) and NASH being uncoupled from insulin resistance. For instance, knockdown on *CGI-58* promotes steatosis yet protects from HFD-associated hepatic insulin resistance (35). Moreover, genetic variants of *PNPLA3* and *TM6SF2* predispose to NASH but not to diabetes and are associated with a higher sensitivity of insulin to inhibit lipolysis (36). Circulating FFAs, but not hepatic TGs, have been reported to be associated with NAFLD (37). The rate of lipolysis, which produces FFA, is increased in the setting of fatty liver (38,39), suggesting that adipose tissue may regulate pathological NAFLD (40). Indeed, removal of epididymal white adipose tissue attenuates the development of fatty and fibrotic liver (41). Collectively, data support the hypothesis that adipose tissue, possibly through lipolysis, regulates some metabolic consequences in liver (41,42). Uncovering the fates of the fatty livers observed here to determine whether retaining hepatic insulin sensitivity in JAK2LA mice influences the ultimate metabolic and pathological outcomes would be interesting.

Our studies have potential limitations that merit comment. First, this work shows, by using gold-standard techniques, that hepatocyte-specific disruption of *Jak2* (JAK2L) leads to severe whole-body and hepatic insulin resistance. However, it is important to consider the differences in body weight and composition between genotypes and the impact on how assessments of glucose homeostasis are performed and normalized. We previously published quantitative magnetic resonance data that reported reductions in lean mass in both JAK2L and JAK2LA mice, which occurs without alterations in food intake, energy expenditure, or ambulatory activity (6). During a hyperinsulinemic-euglycemic clamp, both the dosing of insulin and the normalization of the glucose turnover measurements are typically based on body weight. In obese models, where increases in body weight primarily are due to changes in fat mass, this can result in the inadvertent overdosing of insulin and underestimation of glucose turnover relative to lean mass, as previously discussed (23,43). Of note, in the current studies, plasma insulin values were matched across genotypes during both the chow and the HFD clamps. Furthermore, although normalizing the glucose turnover data to lean mass or per mouse modestly affected the magnitude of the reported differences in some cases, there was no effect on the significance of any of the differences we detected when normalized per kilogram

body weight. Thus, although differences in body weight and fat mass existed between some groups in our studies, the differences did not affect the overall interpretation of the results.

Second, it is important to allow that JAK2 is well known to transduce signals downstream of multiple cytokines other that GH, such as leptin and interleukin-6. As such, although from these and prior experiments we can say definitively that we have abrogated GH signaling, we will need to conduct more-definitive experiments, such as adipocyte-specific deletion of the *Ghr*, to determine whether the phenotypes presented here are entirely attributed to loss of GH signaling.

In summary, concomitant disruption of adipocyte *Jak2* (JAK2LA) corrects both the steatosis and the insulin resistance associated with hepatocyte-only *Jak2* deletion (JAK2L), implicating increased liver lipid as the driver of systemic metabolic abnormalities. However, in the cohort of HFD-fed animals, although JAK2L mice were steatotic and insulin resistant (despite marked reductions in body fat), JAK2LA animals were even more steatotic and yet retained exquisite whole-body and hepatic insulin sensitivity. This strongly suggests that at least on this diet, the liver lipid does not drive the systemic metabolic abnormalities and, instead, that hepatic insulin sensitivity is controlled by adipocyte *Jak2* and correlates with augmented insulin-mediated suppression of FFA. Finally, we show that physiological hepatic insulin resistance is associated with attenuated adipose tissue AKT activity in an adipocyte *Jak2*–dependent manner.

References

1. Nobelprize.org. Bernardo Houssay - Nobel Lecture: The Role of the Hypophysis in Carbohydrate Metabolism and in Diabetes [Internet], 2014. Available from https://www.nobelprize.org/nobel_prizes/medicine/laureates/1947/houssay-lecture.html. Accessed 15 July 2015

2. Greenberg E. Growth hormone and diabetes mellitus. Diabetes 1965;14:43–45

3. Jørgensen JO, Pedersen SA, Thuesen L, et al. Beneficial effects of growth hormone treatment in GH-deficient adults. Lancet 1989;1:1221–1225

4. Takahashi Y, Iida K, Takahashi K, et al. Growth hormone reverses nonalcoholic steatohepatitis in a patient with adult growth hormone deficiency. Gastroenterology 2007;132:938–943

5. Sos BC, Harris C, Nordstrom SM, et al. Abrogation of growth hormone secretion rescues fatty liver in mice with hepatocyte-specific deletion of JAK2 [published correction appears in J Clin Invest 2011;121:3360]. J Clin Invest 2011;121: 1412–1423

6. Nordstrom SM, Tran JL, Sos BC, Wagner KU, Weiss EJ. Disruption of JAK2 in adipocytes impairs lipolysis and improves fatty liver in mice with elevated GH. Mol Endocrinol 2013;27:1333–1342

7. Corbit KC, Camporez JPG, Tran JL, et al. Adipocyte JAK2 mediates growth hormone-induced hepatic insulin resistance. JCI Insight 2017;2:e91001

8. Perry RJ, Camporez JP, Kursawe R, et al. Hepatic acetyl CoA links adipose tissue inflammation to hepatic insulin resistance and type 2 diabetes. Cell 2015;160: 745–758

9. Nielsen S, Møller N, Christiansen JS, Jørgensen JO. Pharmacological anti-lipolysis restores insulin sensitivity during growth hormone exposure. Diabetes 2001; 50:2301–2308

10. Segerlantz M, Bramnert M, Manhem P, Laurila E, Groop LC. Inhibition of the rise in FFA by acipimox partially prevents GH-induced insulin resistance in GH-deficient adults. J Clin Endocrinol Metab 2001;86:5813–5818

11. Fan Y, Menon RK, Cohen P, et al. Liver-specific deletion of the growth hormone receptor reveals essential role of growth hormone signaling in hepatic lipid metabolism. J Biol Chem 2009;284:19937–19944

12. Barclay JL, Nelson CN, Ishikawa M, et al. GH-dependent STAT5 signaling plays an important role in hepatic lipid metabolism. Endocrinology 2011;152: 181–192

13. Barclay JL, Kerr LM, Arthur L, et al. In vivo targeting of the growth hormone receptor (GHR) Box1 sequence demonstrates that the GHR does not signal exclusively through JAK2. Mol Endocrinol 2010;24:204–217

14. Cordoba-Chacon J, Majumdar N, List EO, et al. Growth hormone inhibits hepatic de novo lipogenesis in adult mice. Diabetes 2015;64:3093–3103

15. Wilson CG, Tran JL, Erion DM, Vera NB, Febbraio M, Weiss EJ. Hepatocyte-specific disruption of CD36 attenuates fatty liver and improves insulin sensitivity in HFD-fed mice. Endocrinology 2016;157:570–585

16. Garofalo RS, Orena SJ, Rafidi K, et al. Severe diabetes, age-dependent loss of adipose tissue, and mild growth deficiency in mice lacking Akt2/PKB beta. J Clin Invest 2003;112:197–208

17. Sarbassov DD, Guertin DA, Ali SM, Sabatini DM. Phosphorylation and regulation of Akt/PKB by the rictor-mTOR complex. Science 2005;307:1098–1101

18. Malla R, Wang Y, Chan WK, Tiwari AK, Faridi JS. Genetic ablation of PRAS40 improves glucose homeostasis via linking the AKT and mTOR pathways. Biochem Pharmacol 2015;96:65–75

19. Sancak Y, Thoreen CC, Peterson TR, et al. PRAS40 is an insulin-regulated inhibitor of the mTORC1 protein kinase. Mol Cell 2007;25:903–915

20. Edgerton DS, Kraft G, Smith M, et al. Insulin's direct hepatic effect explains the inhibition of glucose production caused by insulin secretion. JCI Insight 2017;2: e91863

21. Titchenell PM, Chu Q, Monks BR, Birnbaum MJ. Hepatic insulin signalling is dispensable for suppression of glucose output by insulin in vivo. Nat Commun 2015; 6:7078

22. Krempler A, Qi Y, Triplett AA, Zhu J, Rui H, Wagner KU. Generation of a conditional knockout allele for the Janus kinase 2 (Jak2) gene in mice. Genesis 2004;40: 52–57

23. Ayala JE, Samuel VT, Morton GJ, et al.; NIH Mouse Metabolic Phenotyping Center Consortium. Standard operating procedures for describing and performing metabolic tests of glucose homeostasis in mice. Dis Model Mech 2010; 3:525–534

24. Jurczak MJ, Lee AH, Jornayvaz FR, et al. Dissociation of inositol-requiring enzyme (IRE1α)-mediated c-Jun N-terminal kinase activation from hepatic insulin

resistance in conditional X-box-binding protein-1 (XBP1) knock-out mice. J Biol Chem 2012;287:2558–2567

25.   Press M, Tamborlane WV, Sherwin RS. Importance of raised growth hormone levels in mediating the metabolic derangements of diabetes. N Engl J Med 1984; 310:810–815

26.   Holt RI, Simpson HL, Sönksen PH. The role of the growth hormone-insulin-like growth factor axis in glucose homeostasis. Diabet Med 2003;20:3–15

27.   Guevara-Aguirre J, Procel P, Guevara C, Guevara-Aguirre M, Rosado V, Teran E. Despite higher body fat content, Ecuadorian subjects with Laron syndrome have less insulin resistance and lower incidence of diabetes than their relatives. Growth Horm IGF Res 2016;28:76–78

28.   Fukuda I, Hizuka N, Muraoka T, Ichihara A. Adult growth hormone deficiency: current concepts. Neurol Med Chir (Tokyo) 2014;54:599–605

29.   Mittelman SD, Fu YY, Rebrin K, Steil G, Bergman RN. Indirect effect of insulin to suppress endogenous glucose production is dominant, even with hyperglucagonemia. J Clin Invest 1997;100:3121–3130

30.   Michael MD, Kulkarni RN, Postic C, et al. Loss of insulin signaling in hepatocytes leads to severe insulin resistance and progressive hepatic dysfunction. Mol Cell 2000;6:87–97

31.   Titchenell PM, Quinn WJ, Lu M, et al. Direct hepatocyte insulin signaling is required for lipogenesis but is dispensable for the suppression of glucose production. Cell Metab 2016;23:1154–1166

32.   Lee PL, Tang Y, Li H, Guertin DA. Raptor/mTORC1 loss in adipocytes causes progressive lipodystrophy and fatty liver disease. Mol Metab 2016;5: 422–432

33.   Lallukka S, Yki-Järvinen H. Non-alcoholic fatty liver disease and risk of type 2 diabetes. Best Pract Res Clin Endocrinol Metab 2016;30:385–395

34.   Kahn BB, Flier JS. Obesity and insulin resistance. J Clin Invest 2000;106:473–481

35.   Cantley JL, Yoshimura T, Camporez JP, et al. CGI-58 knockdown sequesters diacylglycerols in lipid droplets/ER-preventing diacylglycerol-mediated hepatic insulin resistance. Proc Natl Acad Sci U S A 2013;110:1869–1874

36.   Zhou Y, Llauradó G, Orešič M, Hyötyläinen T, Orho-Melander M, Yki-Järvinen H. Circulating triacylglycerol signatures and insulin sensitivity in NAFLD associated with the E167K variant in TM6SF2. J Hepatol 2015;62:657–663

37.   Liu J, Han L, Zhu L, Yu Y. Free fatty acids, not triglycerides, are associated with non-alcoholic liver injury progression in high fat diet induced obese rats. Lipids Health Dis 2016;15:27

38.   Sunny NE, Parks EJ, Browning JD, Burgess SC. Excessive hepatic mitochondrial TCA cycle and gluconeogenesis in humans with nonalcoholic fatty liver disease. Cell Metab 2011;14:804–810

39.   Armstrong MJ, Hazlehurst JM, Hull D, et al. Abdominal subcutaneous adipose tissue insulin resistance and lipolysis in patients with non-alcoholic steatohepatitis. Diabetes Obes Metab 2014;16:651–660

40.   Bril F, Barb D, Portillo-Sanchez P, et al. Metabolic and histological implications of intrahepatic triglyceride content in nonalcoholic fatty liver disease. Hepatology 2017;65:1132–1144

41.   Mulder P, Morrison MC, Wielinga PY, van Duyvenvoorde W, Kooistra T, Kleemann R. Surgical removal of inflamed epididymal white adipose tissue attenuates the development of non-alcoholic steatohepatitis in obesity. Int J Obes 2016;40:675–684

42.   O-Sullivan I, Zhang W, Wasserman DH, et al. FoxO1 integrates direct and indirect effects of insulin on hepatic glucose production and glucose utilization [published correction appears in Nat Commun 2015;6:7861]. Nat Commun 2015;6:7079

43.   McGuinness OP, Ayala JE, Laughlin MR, Wasserman DH. NIH experiment in centralized mouse phenotyping: the Vanderbilt experience and recommendations for evaluating glucose homeostasis in the mouse. Am J Physiol Endocrinol Metab 2009; 297:E849–E855